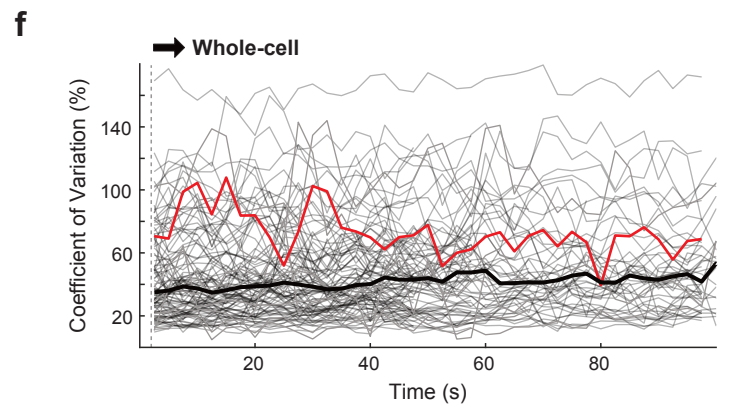
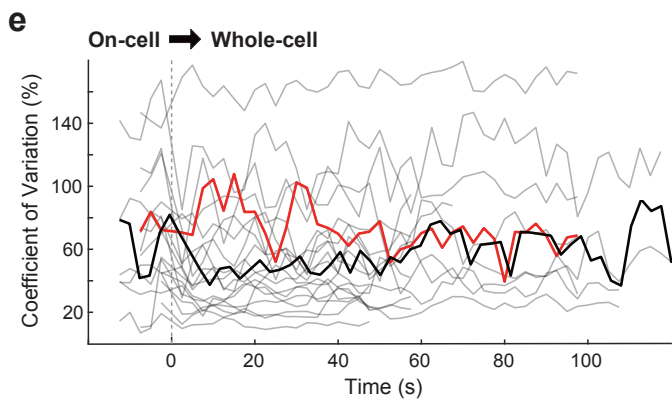
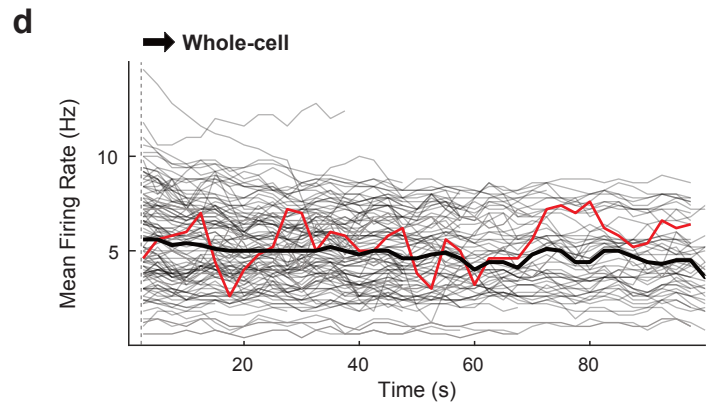
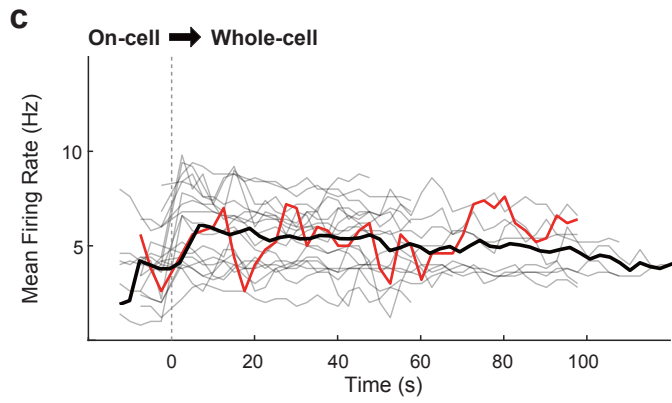
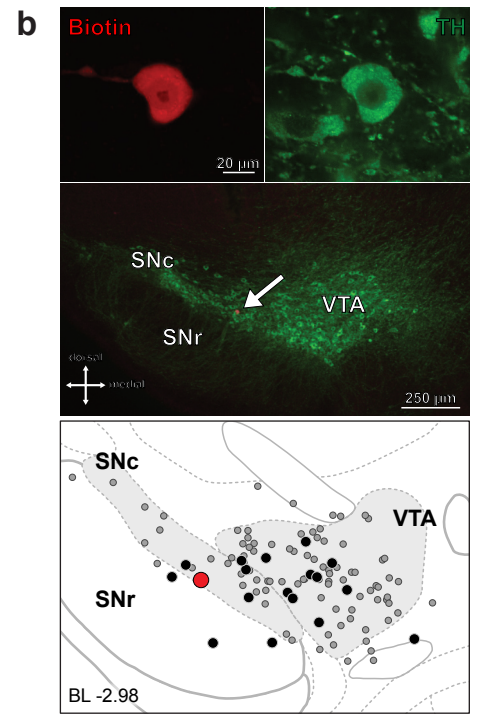
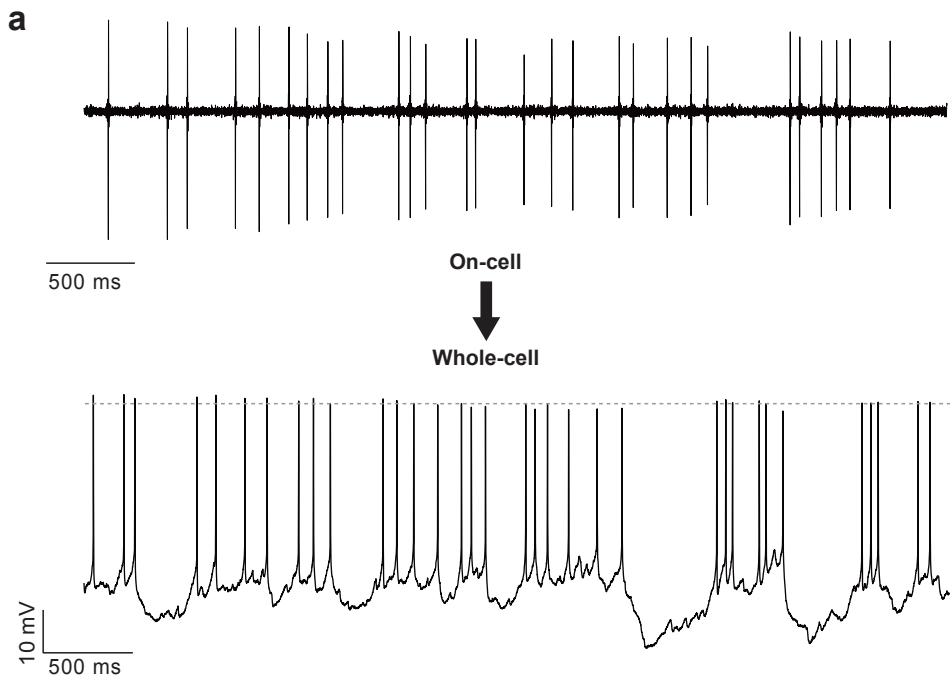
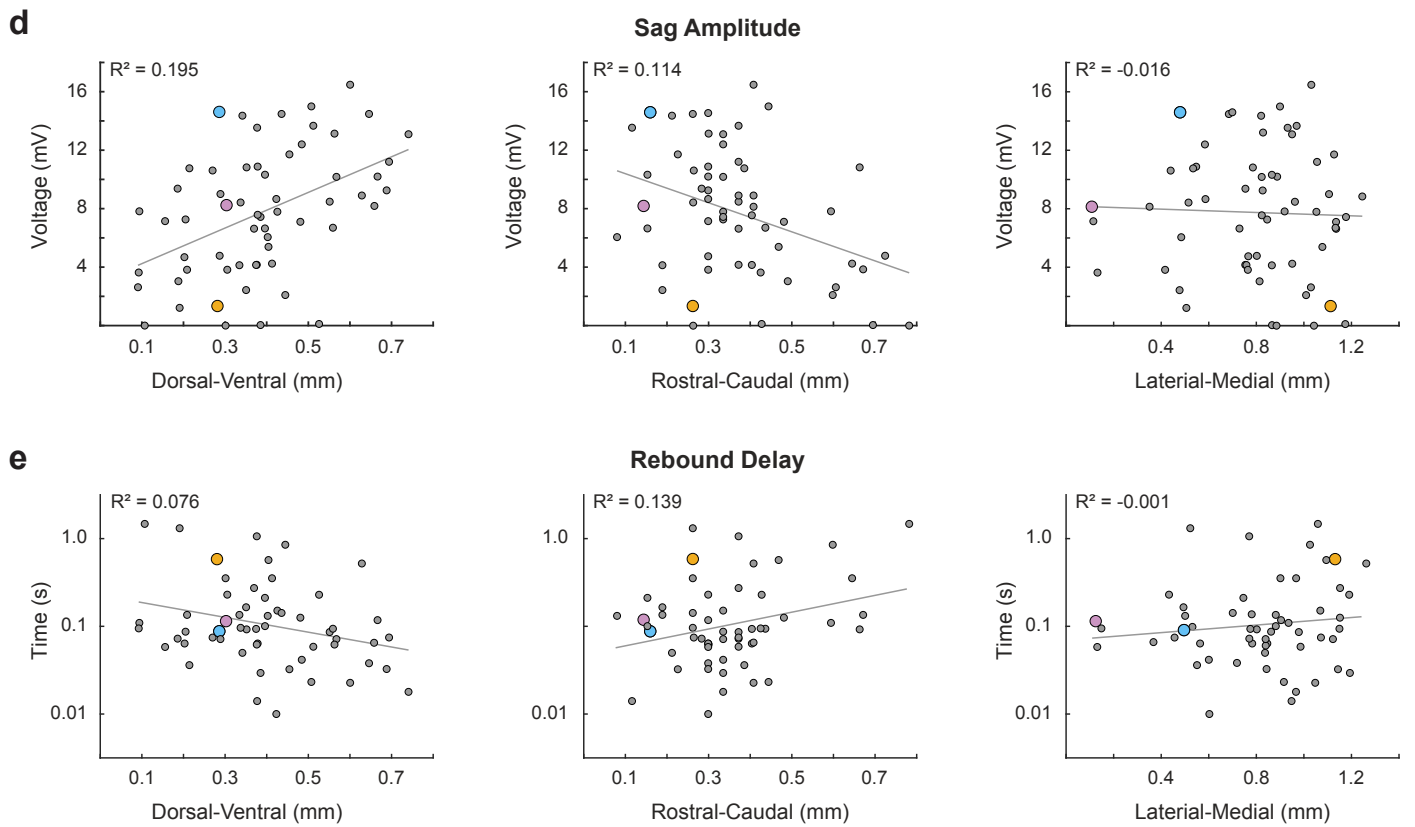
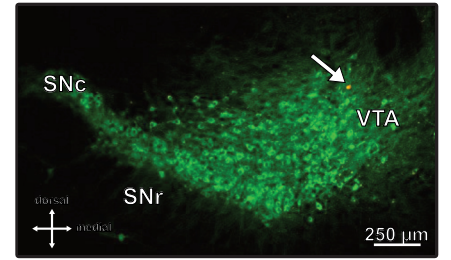
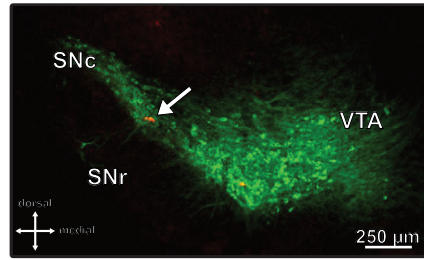
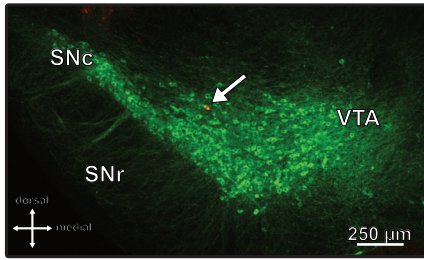
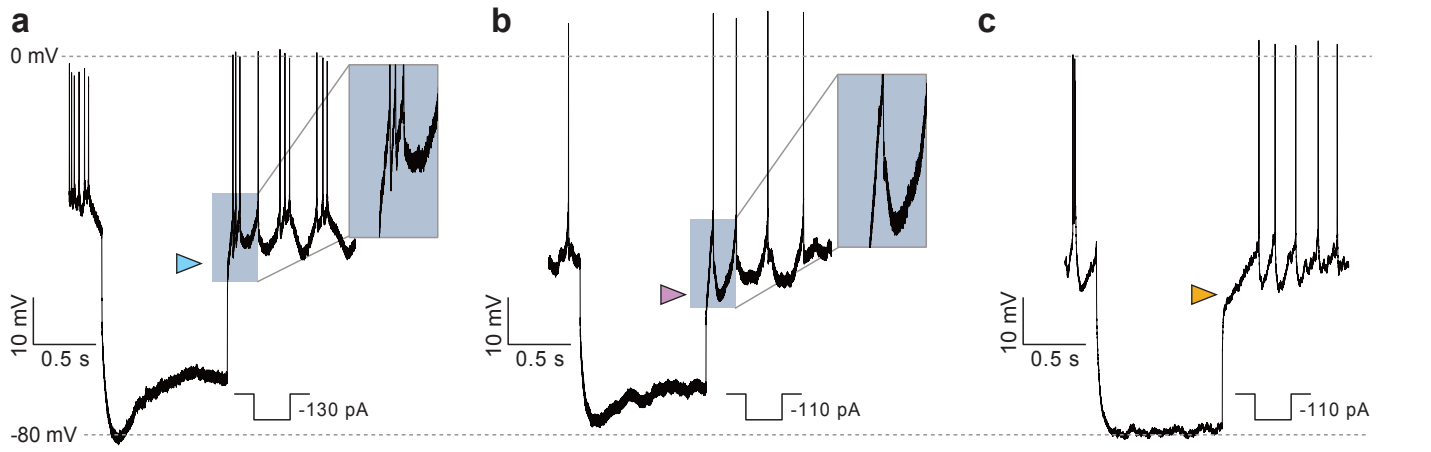


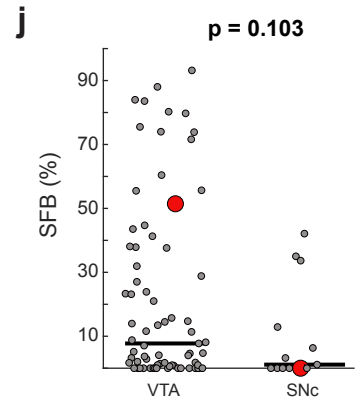
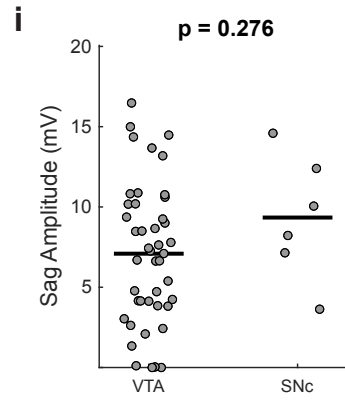
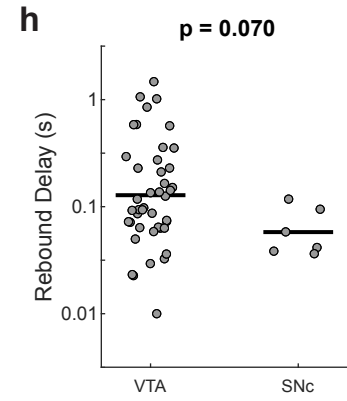
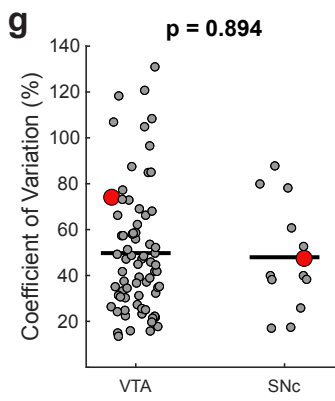
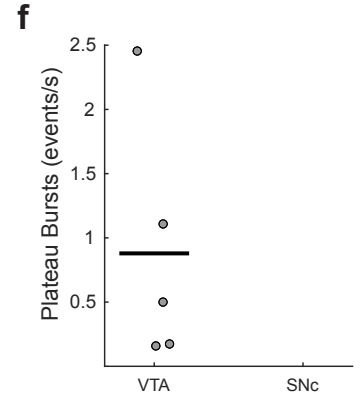
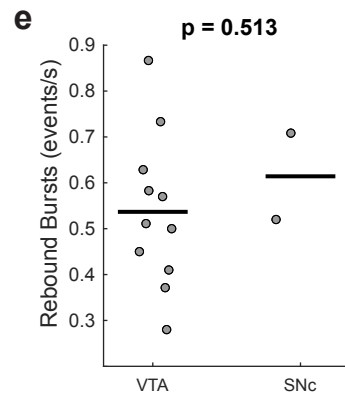
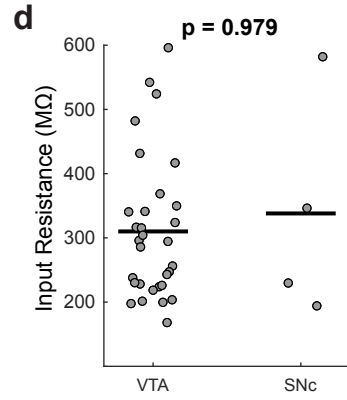
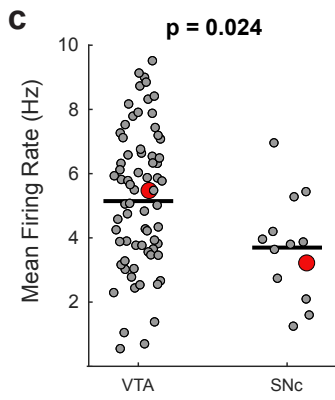
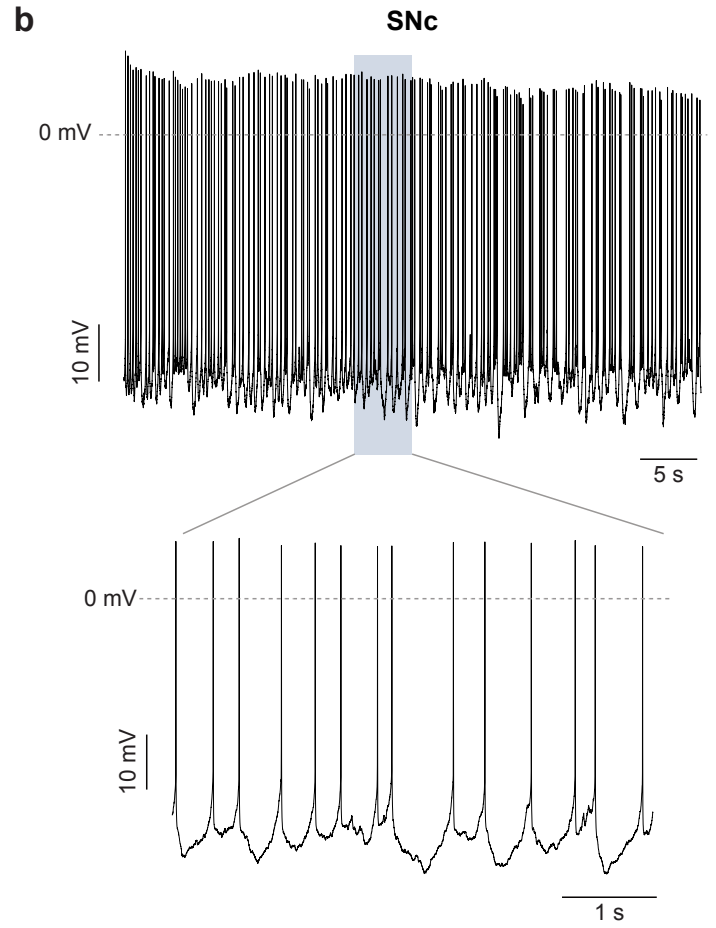
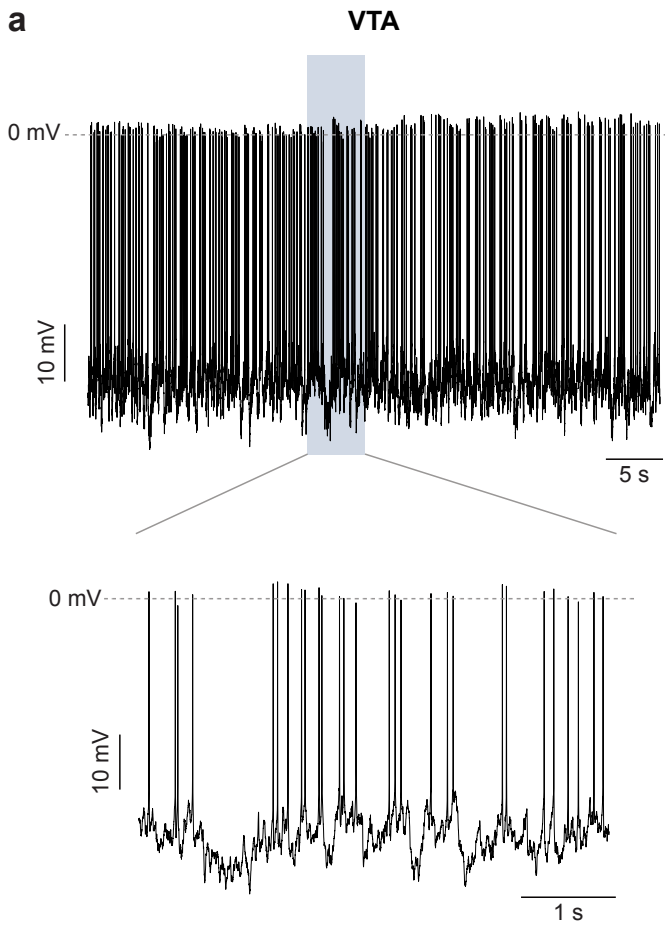
Supplemental Figure 1. Silent and quiet dopamine cells are rare. **a.** Upper trace illustrates the hyperpolarized membrane potential of a dopamine neuron that did not fire spontaneous action potentials. Lower traces illustrate the dopamine neuron firing in response to current injection. **b.** Immunocytochemical identification locates the recorded neuron (arrow) within the SNc. The depiction (lower panel) shows the location of the recorded neuron (large red dot) in relation to all the recorded neurons in this study (black and gray dots). Black dots in B-F represent all cells that fired spontaneously at < 1 spike per minute. **c-f.** Input resistance (**c**), baseline membrane potential (**d**), sag amplitude (**e**), and rebound delay (**f**) of dopamine neurons that fired spontaneously at < 1 spike per minute. Grey dots indicate the same measurements for spontaneously active dopamine neurons.



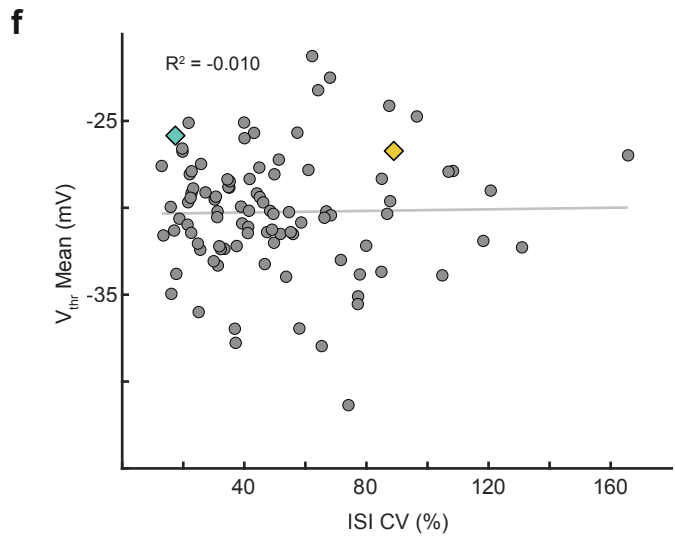
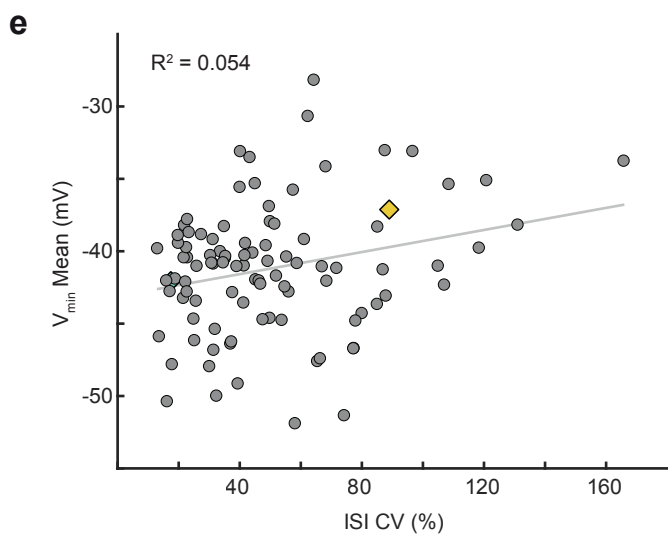
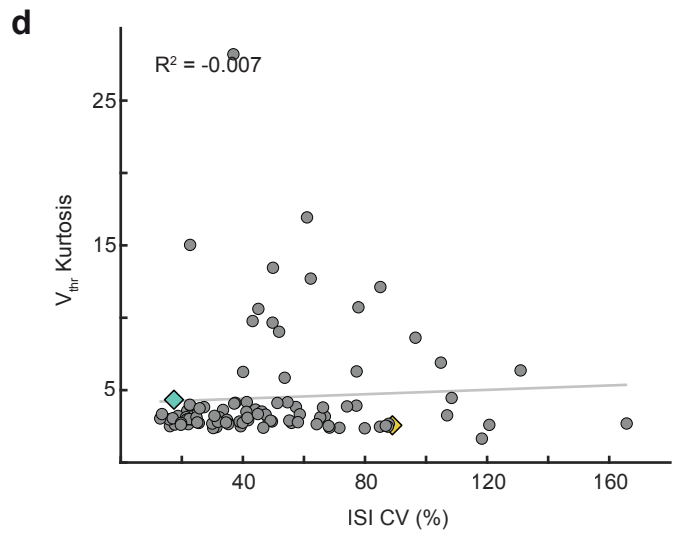
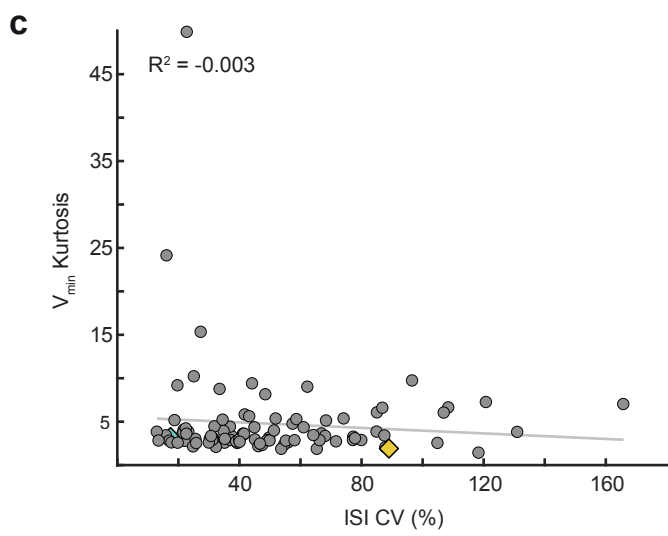
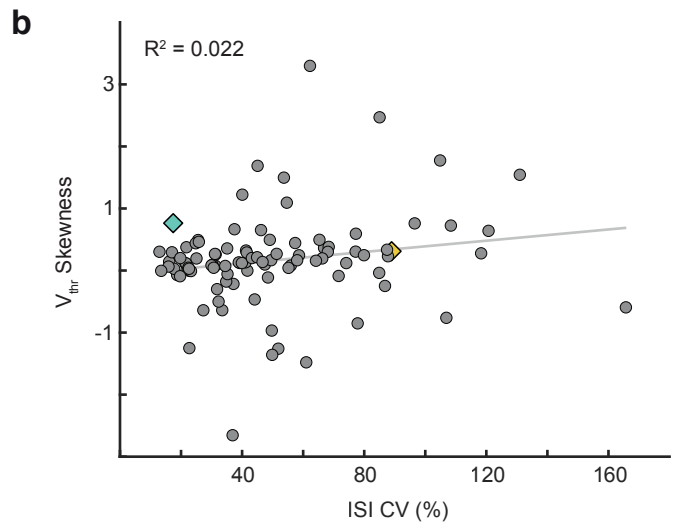
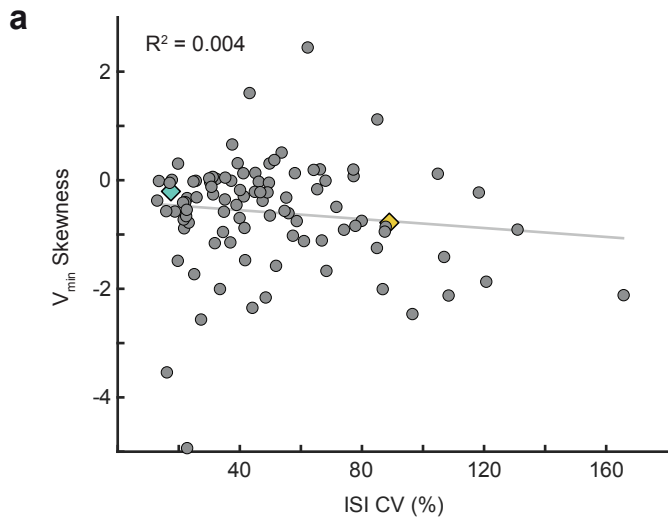
Supplemental Figure 2. *In vivo* whole-cell recording of dopamine neurons does not disturb firing rate or pattern of activity. **a.** Representative recording of spontaneous *in vivo* electrical activity from a neuron recorded in on-cell mode (upper trace) and then broken into the whole-cell configuration (lower trace) with similar firing rate and pattern. **b.** Immunocytochemistry locates the recorded neuron (arrow) within the medial region of the SNc. The depiction (lower panel) shows the location of the recorded neuron (large red dot) in relation to all the recorded neurons in this study (black and gray dots). Black dots represent all cells for which on-cell activity was recorded for comparison with whole-cell activity. **c.** Time series of mean firing rate during the transition from on-cell to whole-cell modes (vertical dashed line at time = 0; change in firing rate from on-cell to whole-cell returns to baseline within 70 seconds of breaking in = -19.86 (-14.86 to -4.36) Hz; $n = 9$, $N = 9$; $p = 0.055$; two-sided Wilcoxon Sign Rank test for paired data). **d.** Time series of mean firing rate for the first 100 seconds from all neurons recorded in this study (slope change in FR = -0.004; $n = 108$, $N = 77$). **e.** Time series of the coefficient of variation (CV) of firing during the transition from on-cell to whole-cell mode (vertical dashed line at time = 0; change in CV from on-cell to whole-cell returns to baseline within 20 seconds of breaking in = -11.75 (-17.7 to 7.26); $n = 19$, $N = 16$; $p = 0.184$; two-sided Wilcoxon Sign Rank test for paired data). **f.** Time series of firing CV for the first 100 seconds from all neurons recorded in this study (slope change in CV = 0.003; $n = 108$, $N = 77$). **c-f.** Red lines represent the example neuron illustrated in A and B. Black lines represent the average of all lines for each panel.



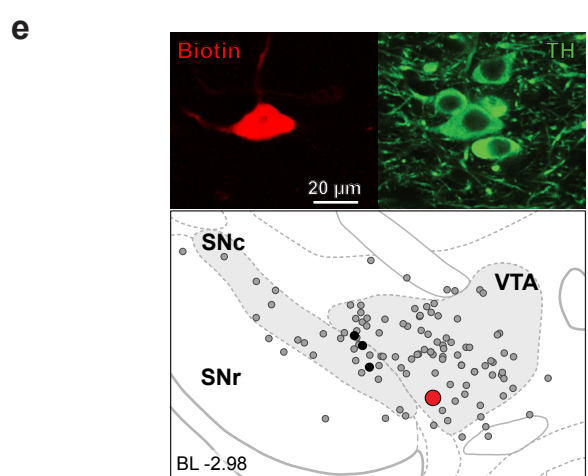
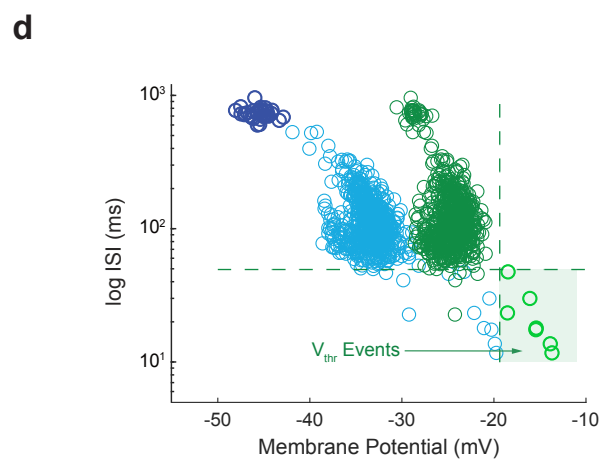
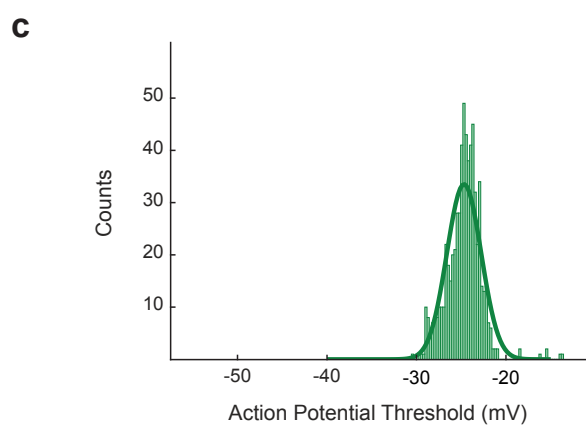
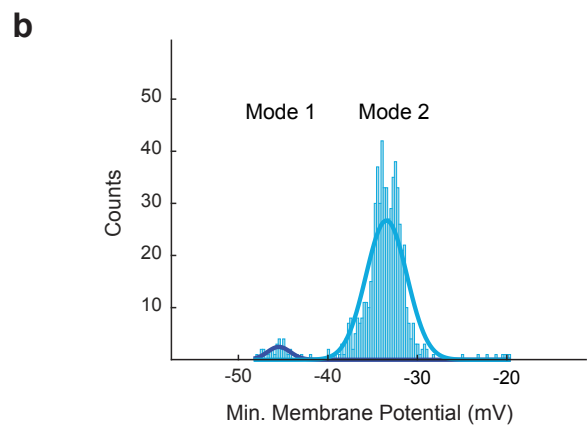
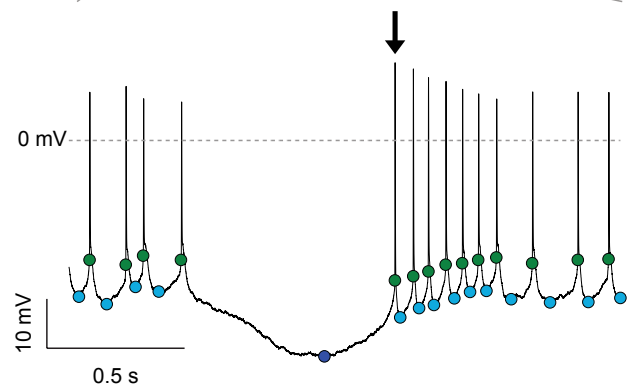
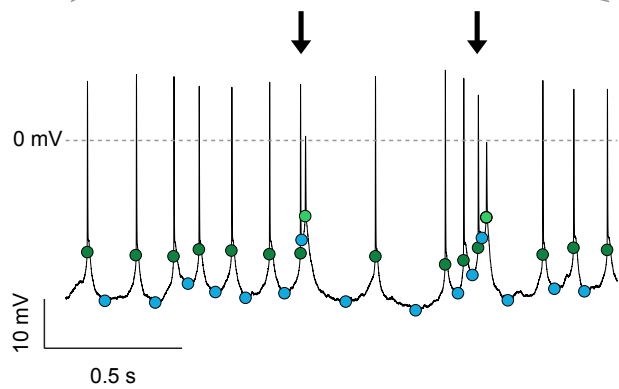
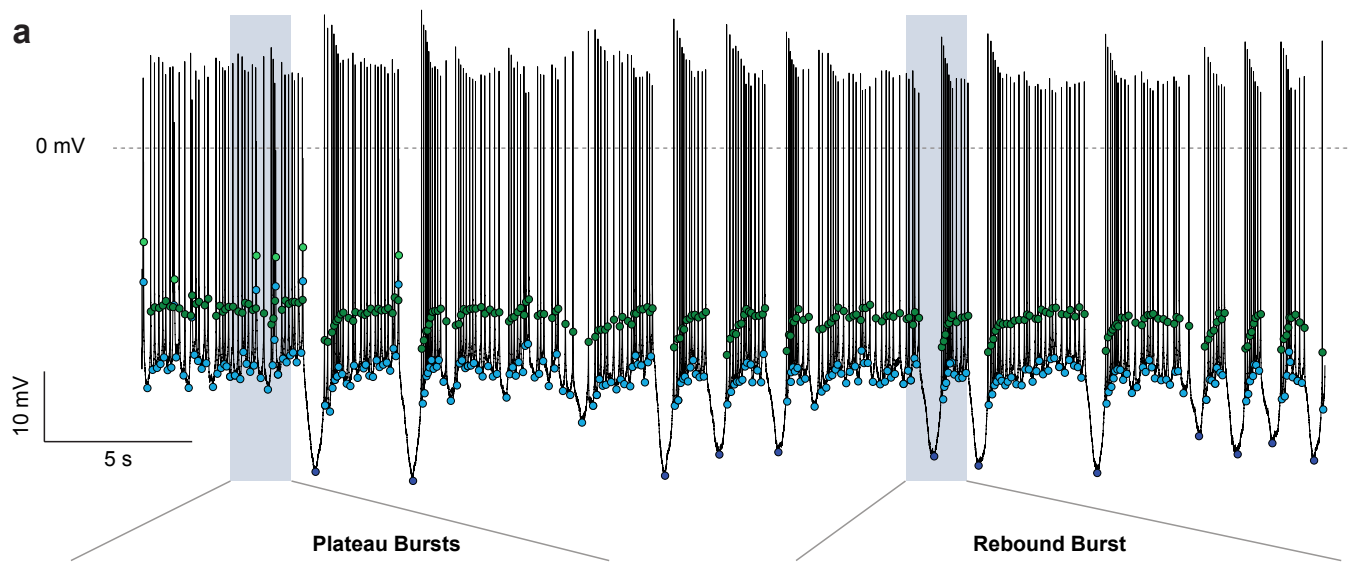
Supplemental Figure 3. Sag and rebound delay are correlated with cell location. **a.** Example recording from an identified dopamine neuron with a large sag in response to hyperpolarizing current injection, and a short delay to the first spike upon removal of the hyperpolarization (blue arrowhead). **a-c.** The immunocytochemical images show the location (arrow) of the recorded neurons. **b.** Example recording from an identified dopamine neuron with a moderate sag in response to hyperpolarizing current injection, and a moderate delay to the first spike upon removal of the hyperpolarization (pink arrowhead). **c.** Example recording from an identified dopamine neuron with almost no sag in response to hyperpolarizing current injection, and a long delay to the first spike upon removal of the hyperpolarization (orange arrowhead). **d,e.** Relationship of cell location with sag amplitude (**d**) and rebound delay (**e**) for all neurons where the relevant protocols were carried out (sag amplitude at -80 mV = 7.8 (4.16 to 10.76) mV, n = 62; N = 53; rebound delay = 92.87 (58.5 to 151.05) ms; n = 58, N = 50). Both measures had a relationship with location in the dorsal-ventral and rostral-caudal planes. Colored dots in panels **d** and **e** correspond to the colored arrowheads in panels **a-c**



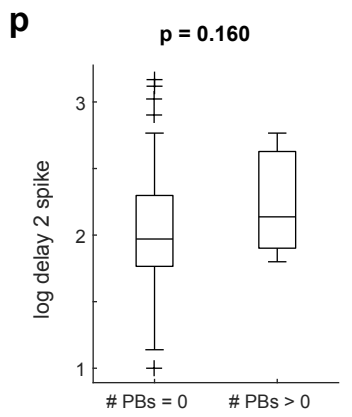
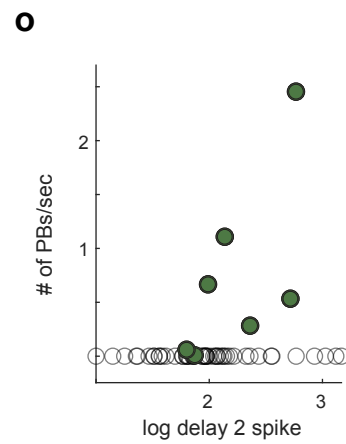
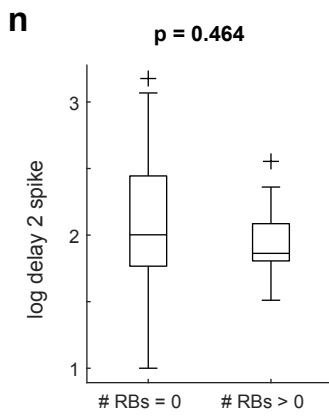
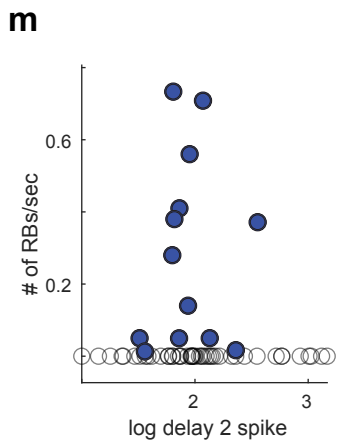
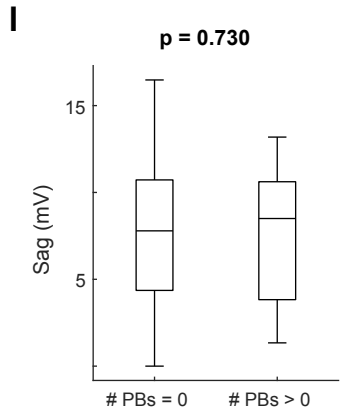
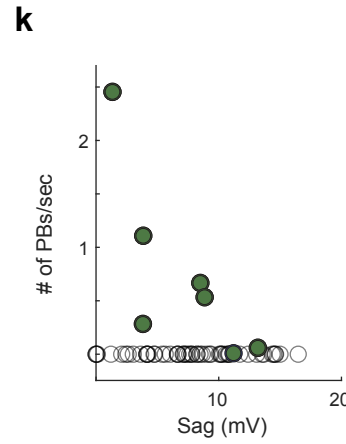
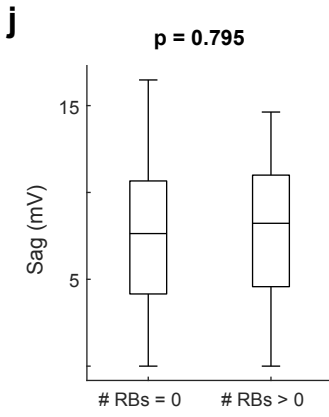
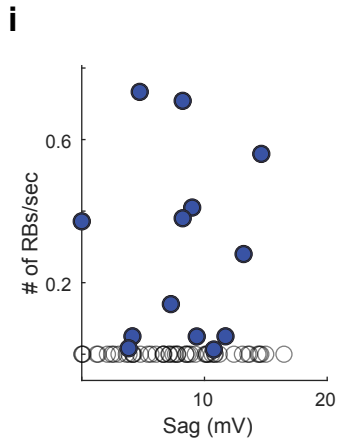
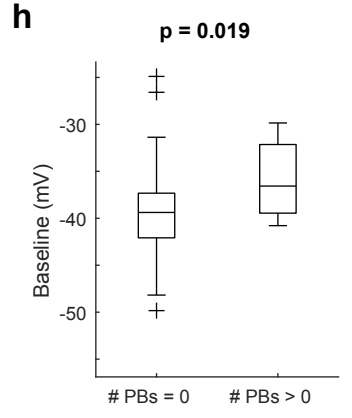
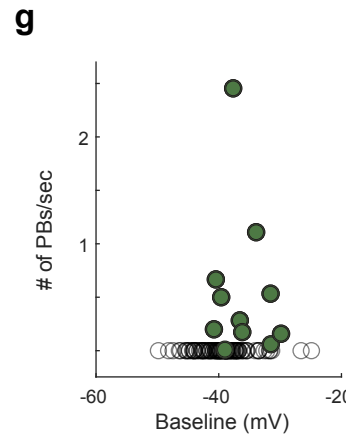
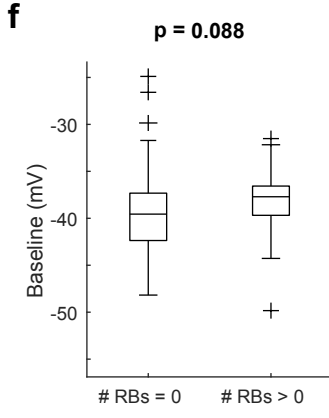
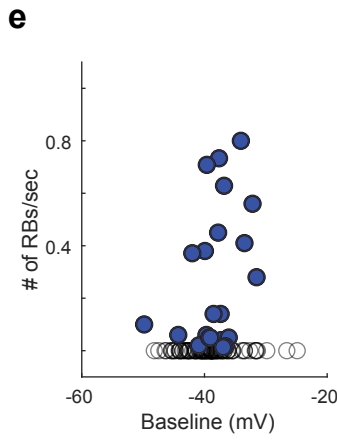
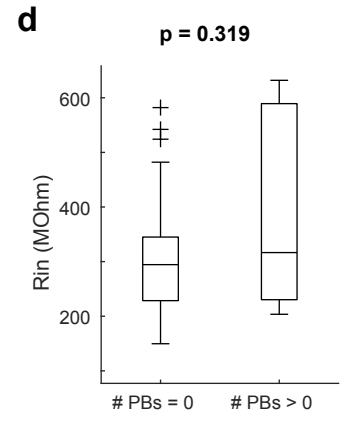
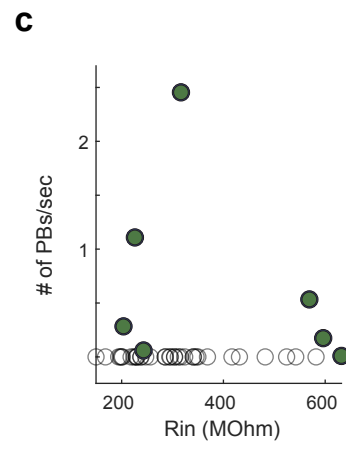
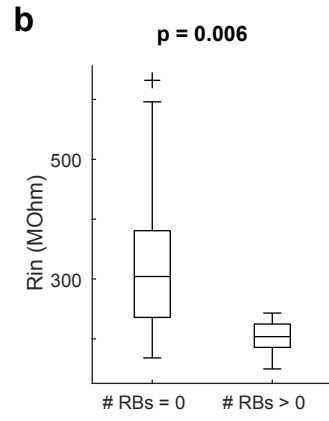
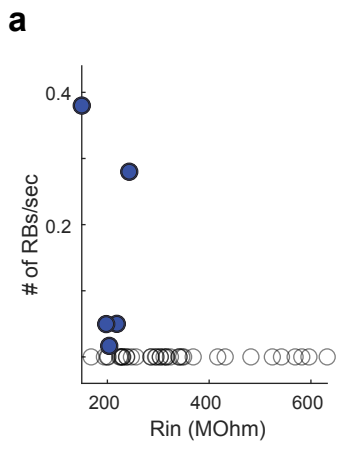
Supplemental Figure 4. SNc and VTA dopamine neurons have similar electrophysiological characteristics *in vivo*. **a, b.** Traces recorded from identified VTA (**a**) and SNc (**b**) dopamine neurons. **c-f.** Mean firing rate (**c**), input resistance (**d**), rebound and plateau burst frequency (**e, f**), ISI CV (**g**), rebound delay (**h**), sag amplitude (**i**), and spikes fired in bursts as determined by the 80/160 ms criterion (**j**) of dopamine neurons located in the VTA and SNc. All analyses are Wilcoxon Rank Sum tests.



Supplemental Figure 5. Spike firing variability does not correlate with general measures of distribution. **a-f.** The coefficient of variation (CV) of the interspike intervals (ISI CV) correlates neither with skewness of the distributions for V_{\min} (**a**) or V_{thr} (**b**), kurtosis of distributions for V_{\min} (**c**) or V_{thr} (**d**), nor mean membrane potential of V_{\min} (**e**) or V_{thr} (**f**; $n = 97$, $N = 72$). Cyan and yellow diamonds depict the values for the example cells illustrated in Figure 2 and the highlighted ISI CV in Figure 1f.



Supplemental Figure 6. Dopamine neurons can fire both rebound and plateau bursts during a single recording. **a.** Trace of a recording from an identified dopamine neuron. Lower traces illustrate examples of plateau bursts (left lower trace) and a rebound burst (right lower trace). **b, c.** Distributions for V_{\min} (**a**), displaying a bimodal distribution; and V_{thr} (**b**) displaying a unimodal distribution. **d.** Scatter Plot of ISI versus V_{\min} and V_{thr} . Green dashed lines indicate outlier identification in the lower left plane for V_{thr} with detected events in the shaded region. Dark blue circles identified from Mode 1 in panel **b**. **e.** Immunocytochemical identification and location (red dot).



Supplemental Figure 7. Comparison of dopamine neurons with or without bursts. **a-d.** Input resistance of dopamine neurons with and without (rebound burst grey circles; n = 35, N = 33; plateau burst grey circles; n = 33, N = 30) rebound bursts (blue dots; **a, b**; n = 5, N = 5) or plateau bursts (green dots; **c, d**). **e-h.** Baseline membrane potential of dopamine neurons with and without rebound bursts (**e, f**; rebound burst grey circles; n = 88, N = 66; plateau burst grey circles; n = 98, N = 73; blue dots n = 22, N = 21) or plateau bursts (**g, h**; n = 12, N = 12). **i-l.** Sag amplitude of dopamine neurons with and without rebound bursts (**i, j**; rebound burst grey circles; n = 47, N = 43; plateau burst grey circles; n = 52, N = 47; blue dots n = 13, N = 13) or plateau bursts (**k, l**; n = 8, N = 8). **m-p.** Delay to first spike from hyperpolarization of dopamine neurons with and without rebound bursts (**m, n**; rebound burst grey circles; n = 46, N = 42; plateau burst grey circles; n = 51, N = 46; blue dots n = 13, N = 13) or plateau bursts (**o, p**; n = 8, N = 8). Box plots are 25th (q1), 50th (q2) and 75th (q3) percentiles. Whiskers are $q1 - 1.5 \times (q3 - q1)$ and $q3 + 1.5 \times (q3 - q1)$. Points outside the whisker range are plotted individually. All comparisons done using a two-sided Wilcoxon Rank Sum test.

Supplemental Data Table 1

Table showing that there were no significant differences in firing rate and CV of ISI between various groupings of cells:

- Cell from animals belonging to sub-strains C57BL/6N vs C57BL/6J
- Cells from male vs female animals
- Recordings made using internal solution containing 40 nM vs 80 nM free calcium

All values are reported as median (25th quantile-75th quantile), and all p-values are reported for the Wilcoxon rank sum test. Upper-case letter 'N' indicates the number of animals and the lower-case letter 'n' indicates the number of cells in that grouping.

Comparison type	FR (Hz)			CV		
	N	J	p-value	N	J	p-value
C57BL/6N (n=90, N=64) vs C57BL/6J (n=20, N=15)						
	5.17 (3.56-6.96)	5.39 (3.61-6.62)	0.83	41 (26 - 64) %	49 (39 - 68) %	0.14
Male (n=98, N=72) vs Female (n=12, N=7)	m	f	p-value	m	f	p-value
	5.07 (3.56-6.58)	6.07 (4.38-7.2)	0.23	0.41 (0.26-0.66)	0.45 (0.41-0.58)	0.32
[Ca⁺⁺] 40nM (n=7, N=5) vs 80nM (n=103, N=74)	40	80	p-value	40	80	p-value
	4.25 (1.8-6.4)	5.27 (3.63-6.88)	0.33	0.45 (0.38-0.75)	0.42 (0.3-0.65)	0.72

Supplemental Data Table 2

Table comparing different measures taken from *in vivo* and *in vitro* whole-cell recordings, and *in vivo* juxtacellular recordings. All values are reported as median (25th quantile-75th quantile), and all p-values are reported for the Wilcoxon rank sum test.

Input Resistance (MΩ)		
In Vivo Whole-cell (n = 42)	In Vitro Whole-cell (n = 71)	p-value
295.2 (227.6-354.5)	443.1 (288.1-641.7)	<0.0001
80/160 SFB (%)		
In Vivo Whole-cell (n = 110)	In Vivo Juxtacellular (n = 102)	p-value
9.81 (0.755-38.5)	1.48 (0.113-9.30)	0.0007
Firing Rate (Hz)		
In Vivo Whole-cell (n = 110)	In Vivo Juxtacellular (n = 102)	p-value
5.25 (3.54-6.81)	3.16 (2.22-4.31)	<0.0001
CV (%)		
In Vivo Whole-cell (n = 110)	In Vivo Juxtacellular (n = 102)	p-value
42.5 (30.2-65.6)	49.7 (31.8-73.0)	0.1031

Supplemental Data Table 3

Table showing trajectories of repolarization speed (min dV/dt) across three types of spiking activity patterns. All values are reported as median (25th quantile-75th quantile), and all p-values are reported for the Wilcoxon rank sum test.

Spiking pattern	min dV/dt spike 1 vs spike 2 (V/s)		min dV/dt spike 2 vs spike 3 (V/s)	
	Magnitude	p-value	Magnitude	p-value
Pacemaker	0.003 (-0.0066 to 0.012)	0.38	-0.082 (8.95x10 ⁻⁵ to 0.017)	0.19
	Magnitude	p-value	Magnitude	p-value
Rebound burst	-6.85 (-10.97 to -5.63)	0.002	2.87 (2.19 to 3.08)	0.002
	Magnitude	p-value	Magnitude	p-value
Plateau burst	0.53 (-0.2 to 1.77)	0.7	7.16 (5.34 to 8.31)	0.002
	Magnitude	p-value	Magnitude	p-value
Mixed pattern rebound	-3.91 (-4.73 to -3.17)	4.88x 10 ⁻⁴	1.29 (0.94 to 1.76)	4.88x10 ⁻⁴
	Magnitude	p-value	Magnitude	p-value
Mixed pattern plateau	0.74 (0.043 to 1.38)	0.5	5.81 (0.28 to 11.33)	0.5